Hydrothermal Synthesis and Characterization of the New Layered Fluorogallophosphate Mu-23

Ludovic Josien,[a] Angélique Simon-Masseron,*[a] Volker Gramlich,[b] and Joël Patarin[a]

Abstract: Mu-23, $[(C_6H_{15}N_2)(C_6H_{16}N_2)Ga_5F_6(H_2O)_2(PO_4)_4]\cdot 4H_2O$, the first layered fluorinated gallophosphate with a Ga/P molar ratio of 5:4, was obtained in the presence of fluoride ions with 1,4-dimethylpiperazine as an organic template. It crystallizes in the triclinic space group $P\bar{1}$ (no. 2) with unit cell parameters $a=8.735(11)$, $b=8.864(5)$, $c=12.636(10)$ Å, $\alpha=98.36(5)$, $\beta=100.18(8)$, $\gamma=115.84(7)^\circ$. The layers consist of $GaO_2F_3(H_2O)$, GaO_4F_2 octahedra, and GaO_4 and PO_4 tetrahedra; these moieties share their oxygen and some of their fluorine atoms. The connectivity scheme of these different polyhedra leads to the formation of eight-membered rings.

Keywords: dimethylpiperazine · fluorides · gallium · gallophosphates · layered compounds · structure elucidation

Introduction

Open-framework metal phosphates, like the well-known zeolites (i.e., microporous aluminosilicates), have attracted research activities because of their potential applications.[1] Three-dimensional frameworks with large pores, such as the aluminophosphates VPI-5 with 18-membered rings (18MR)[2] and JDF-20 (20MR),[3] the gallophosphate NTHU-1 (24MR),[4] and the zincophosphate ND-1 (24MR) [5] have been investigated. Typically these materials are prepared under hydrothermal or solvothermal conditions. The introduction by Guth et al. of fluoride ions in the synthesis mixture has opened a route for synthesizing new microporous fluorinated metal phosphates.[6] For example, the ferrophosphate $[Fe_5F_4(H_2PO_4)(HPO_4)_3(PO_4)_3](C_4H_{13}N_3)_2\cdot H_2O$ (24MR),[7] the nickel phosphate VSB-1 (24MR),[8] and the gallophosphate cloverite (20MR)[9] have been prepared in fluoride media. In these as-synthesized materials, fluorine is part of the framework as bridging and terminal species. It can also be trapped into the so-called double-four ring units (D4R).

Table 1. Gallophosphates with a Ga/P ratio higher than one.

Name	Structure-directing species	Chemical formula	Ga/P ratio	Reference
[a]	sodium	$[Na_3Ga_5(PO_4)_4O_2(OH)_2]\cdot 2H_2O$	5:4	[10]
[a]	4,4′-bipyridine	$[Ga_5(OH)_2(C_2O_4)(PO_4)_4(C_{10}H_9N_2)]\cdot 2H_2O$	5:4	[11]
Mu-5	cyclam[b]	$[Ga_{16}P_{16}O_{64}F_8(OH)_4(GaC_{10}H_{24}N_4)_4]$	5:4	[12]
ULM-2	DABCO[c]	$[Ga_8P_6O_{24}F_4(OH)_4(C_6N_2H_{14})]\cdot 4H_2O$	4:3	[13]
dipyr-GaPO	4,4′-bipyridine	$[Ga_7P_6O_{28}F_3(C_{10}N_2H_{16})]$	7:6	[14]
Mu-23	DMPIP[d]	$[(C_6H_{15}N_2)(C_6H_{16}N_2)Ga_5F_6(H_2O)_2(PO_4)_4]\cdot 4H_2O$	5:4	this work

[a] Not specified. [b] Cyclam = 1,4,8,11-tetraazacyclotetradecane. [c] DABCO = diazabicyclo[2.2.2]octane. [d] DMPIP = 1,4-dimethylpiperazine.

In most gallophosphates and whatever the dimensionality of the inorganic network, the molar ratio Ga/P ≤ 1. Only five three-dimensional structures display a Ga/P molar ratio higher than one (see Table 1): 1) a gallophosphate templated with a sodium cation which is characterized by a Ga/P ratio of 5:4;[10] 2) an oxalate–gallophosphate in which a $C_2O_4^{2-}$ group takes the place of a PO_4 group, reducing the number of P atoms in the structure and increasing the Ga/P ratio to 5:4;[11] 3) the fluorogallophosphate Mu-5, which contains a Ga–cyclam complex that increases the Ga/P ratio to 5:4 instead of 1:1;[12] 4) the fluorogallophosphate ULM-2, with a Ga/P ratio 4:3;[13] and 5) the fluorogallophosphate dipyr-GaPO,[14] with a Ga/P ratio 7:6. All these materials have a three-dimensional framework. To our knowledge, no layered or chain-like structure with a Ga/P molar ratio higher than one has been reported in the literature.

Here we report the synthesis and characterization of the first layered gallophosphate with a Ga/P ratio higher than one.

[a] Dr. A. Simon-Masseron, L. Josien, Dr. J. Patarin
Laboratoire de Matériaux Minéraux UMR 7016
Université de Haute-Alsace
3 rue Alfred Werner, 68093 Mulhouse Cedex (France)
Fax: (+33) 3-89-33-68-85
E-mail: a.simon@uha.fr

[b] Prof. Dr. V. Gramlich
Laboratorium für Kristallographie, ETH-Zentrum
Sonneggstrasse 5, 8092 Zürich (Switzerland)

  0947-6539/02/0807-1614 $ 20.00+.50/0

This material, Mu-23, was prepared from a fluorine-containing mixture in the presence of 1,4-dimethylpiperazine (DMPIP) as an organic template. The material was characterized by X-ray diffraction, chemical analysis, thermal analysis, and solid-state NMR spectroscopy. The single-crystal structure determination is also reported.

Results and Discussion

Synthesis and crystal morphology: Mu-23 crystallizes in a narrow range of synthesis conditions (Table 2), and the amounts of Ga and amine are critical to obtain a pure Mu-23 phase. The Ga/P ratio in Mu-23 (5:4) is quite different from that in the starting mixture (SM), that is, $(Ga/P)_{SM} = 1{:}4$ (sample A, Table 2). Surprisingly, attempts to increase the $(Ga/P)_{SM}$ ratio induce the co-crystallization of an unidentified phase (INC), which is obtained pure when $(Ga/P)_{SM}$ reaches 1:1 (samples B and C, Table 2). 1,4-Dimethylpiperazine (DMPIP) loses its templating effect when it is present in large amounts; this leads to amorphous materials (sample D, Table 2).

Table 2. Syntheses performed in the $x\,Ga_2O_3/4\,P_2O_5/8\,HF/640\,H_2O/y$ DMPIP system at 130 °C during a six-day period.

Sample	x	y	XRD results
A	1	8	Mu-23
B	2	8	Mu-23 + INC[a]
C	4	8	INC
D	1	16	amorphous GaOOH

[a] Major phase.

Mu-23 samples consist of large spheres of aggregated crystals (sphere diameter up to 2 mm). A broken sphere is shown in Figure 1. Individual crystals display rhomboidal prism morphology and their sizes range from $75 \times 50 \times 30$ μm to $700 \times 500 \times 200$ μm.

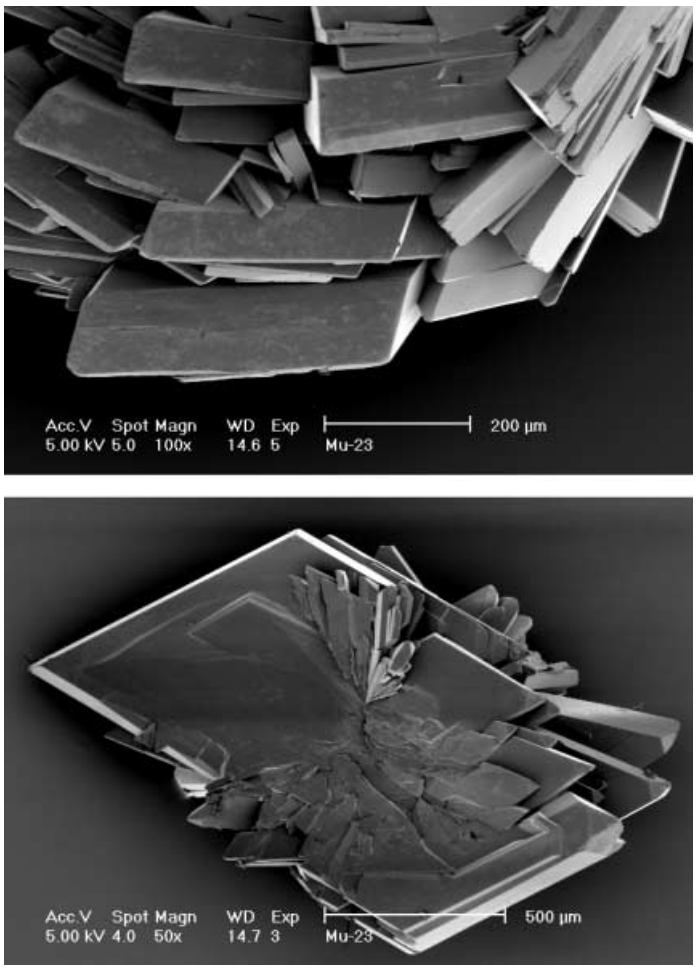

Figure 1. Scanning electron micrographs of the fluorogallophosphate Mu-23.

Structure determination: The powder X-ray diffraction (XRD) pattern of Mu-23 (Figure 2a) was indexed in the triclinic symmetry, space group $P\bar{1}$ (no. 2) with unit cell parameters $a = 8.735(11)$, $b = 8.864(5)$, $c = 12.636(10)$ Å, $\alpha = 98.36(5)$, $\beta = 100.18(8)$, $\gamma = 115.84(7)^\circ$; for comparison, see the XRD pattern of the unknown phase INC (Figure 2c).

For the structure determination, a single crystal with dimensions $0.4 \times 0.4 \times 0.2$ mm was selected. A total number of 2975 independent reflections were recorded ($2.64 \leq \theta \leq 25.05^\circ$) for which 2432 fulfilled the condition $I > 2\sigma(I)$. The experimental and crystallographic data are summarized in Table 3.

From direct methods by using SHELXS-86,[15] the positions of Ga and P atoms were revealed. All the remaining atoms, except H, were located from successive Fourier maps by using SHELXL-93.[16] Hydrogen atoms were placed with geometrical constraints. The resulting atomic coordinates including the equivalent isotropic displacement parameters are reported in Table 4, and selected bond lengths and angles in Tables 5 and 6 respectively. The non-hydrogen atoms were refined with

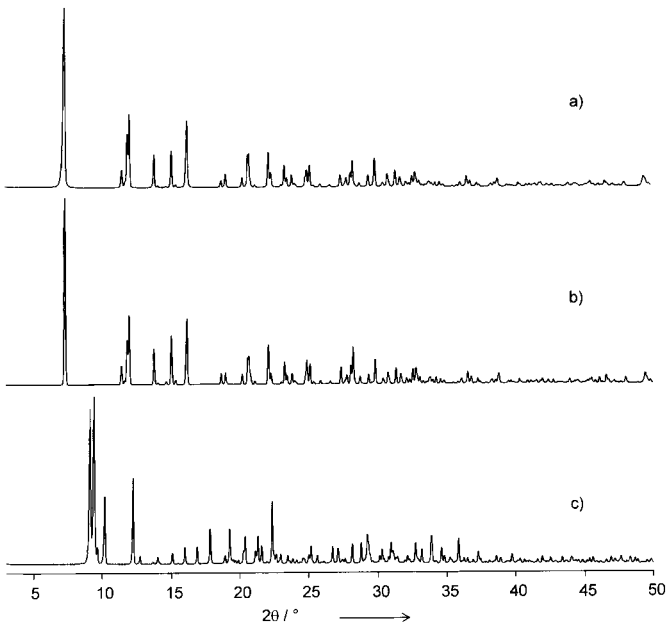

Figure 2. a) Experimental XRD pattern of Mu-23. b) Simulated XRD pattern of Mu-23 calculated from the single-crystal structure data. c) Experimental XRD pattern of phase INC.

Table 3. Experimental and crystallographic data for the fluorogallophosphate Mu-23.

formula	$[(C_6H_{15}N_2)(C_6H_{16}N_2)$-$Ga_5F_6(H_2O)_2(PO_4)_4]\cdot 4H_2O$
crystal system	triclinic
crystal space group	$P\bar{1}$
a [Å]	8.735(11)
b [Å]	8.864(5)
c [Å]	12.636(10)
α [°]	98.36(5)
β [°]	100.18(8)
γ [°]	115.84(7)
M_r [g mol^{-1}]	1181.97
ρ_{calcd}	2.340
V [Å^3]	838.9(13)
Z	1
crystal size [μm]	$400\times400\times200$
λ [Å] ($Mo_{K\alpha}$)	0.71073
μ [mm^{-1}]	4.280
absorption correction	integration
max/min transmission	0.46/0.26
$F(000)$	588
T [K]	293(2)
θ range [°]	2.64–25.05
index ranges	$-10\le h\le 10$
	$-10\le k\le 10$
	$0\le l\le 15$
independent reflections	2975
observed reflections [$I>2\sigma(I)$]	2432
data/restraints/parameters	2975/18/247
residuals (observed data) [$I>2\sigma(I)$]	$R_1=0.0255$, $wR_2=0.0641$
residuals (all data)	$R1=0.0304$, $wR2=0.0652$
goodness-of-fit (all data)	0.975
largest diff. peak/hole [e Å^{-3}]	0.659/−0.905

Table 4. Atomic coordinates and equivalent isotropic displacement parameters [Å^2] for the fluorogallophosphate Mu-23 (standard deviations are in parentheses).

Atom	x	y	z	U_{eq}
Ga1	0	0.5	0	0.00893(12)
Ga2	0.27456(5)	0.03080(4)	0.00642(3)	0.0971(10)
Ga3	0.73844(5)	0.37774(5)	−0.27681(3)	0.01065(11)
P1	0.60563(11)	0.22351(11)	−0.07886(7)	0.0097(2)
P2	0.09343(11)	0.24599(10)	0.10892(7)	0.0093(2)
O1	0.0718(3)	0.3216(3)	0.0113(2)	0.0121(5)
O2	−0.0936(3)	0.1177(3)	0.1159(2)	0.0127(5)
O3	0.1911(3)	0.3793(3)	0.2189(2)	0.0136(5)
O4	0.1917(3)	0.1410(3)	0.0939(2)	0.0155(5)
O5	0.3882(3)	−0.0501(3)	0.0988(2)	0.0151(5)
O6	0.4394(3)	0.1950(3)	−0.0410(2)	0.0148(5)
O7	0.5859(3)	0.2800(3)	−0.1855(2)	0.0142(5)
O8	0.6693(3)	0.1434(3)	−0.3506(2)	0.0177(6)
O9	0.2324(3)	0.6451(3)	−0.0122(2)	0.0126(5)
OW1	0.6952(4)	0.0253(4)	0.4511(2)	0.0311(7)
OW2	0.8770(4)	0.2280(4)	0.3290(3)	0.0399(8)
F1	0.9331(2)	0.4031(2)	−0.1601(2)	0.0136(4)
F2	0.9032(3)	0.4362(3)	−0.3618(2)	0.0184(5)
F3	0.5600(3)	0.3730(3)	−0.3836(2)	0.0187(4)
N1	−0.1090(4)	0.7169(4)	0.3029(3)	0.0235(7)
N4	−0.4156(4)	0.4343(4)	0.3329(3)	0.0203(7)
C5	−0.2517(5)	0.5414(5)	0.4258(3)	0.0234(9)
C2	−0.2720(5)	0.6120(5)	0.2109(3)	0.0261(9)
C3	−0.3707(5)	0.4324(5)	0.2243(3)	0.0257(9)
C6	−0.1551(5)	0.7212(5)	0.4114(3)	0.0249(9)
C7	−0.5160(6)	0.2550(5)	0.3455(4)	0.0326(10)
C8	−0.0124(6)	0.8945(6)	0.2886(5)	0.0417(12)

Table 5. Selected bond lengths [Å] for the fluorogallophosphate Mu-23.[a]

Ga1−O9#1	1.921(3)	P1−O7	1.512(3)
Ga1−O1#1	1.952(2)	P1−O9#3	1.510(3)
Ga1−F1#2	1.953(3)	P1−O6	1.537(3)
Ga2−O6	1.812(3)	P1−O5#5	1.547(2)
Ga2−O4	1.812(3)	P2−O1	1.508(3)
Ga2−O5	1.821(3)	P2−O3	1.509(3)
Ga2−O2#4	1.830(3)	P2−O4	1.530(3)
Ga3−F3	1.854(3)	P2−O2	1.559(3)
Ga3−F2	1.885(3)		
Ga3−O7	1.920(3)	N1−C2	1.480(5)
Ga3−O8	1.921(3)	N1−C8	1.484(5)
Ga3−O3#3	1.944(3)	N1−C6	1.495(5)
Ga3−F1	1.949(3)	N4−C7	1.492(5)
		N4−C5	1.492(5)
O8···OW1	2.659(6)	N4−C3	1.493(5)
OW1···O2W	2.705(6)		
OW2···F2	2.664(6)	C2−C3	1.497(6)
N1···F2	2.752(4)	C5−C6	1.501(6)
N4···F3	2.601(4)		

[a] Symmetry transformation used to generate equivalent atoms: #1: $-x$, $-y+1$, $-z$; #2: $x-1$, y, z ; #3: $-x+1$, $-y+1$, $-z$; #4: $-x$, $-y$, $-z$; #5: $-x+1$, $-y$, $-z$.

Table 6. Selected angles [°] of the fluorogallophosphate Mu-23.[a]

O9-Ga1-O9#1	180.0	F3-Ga3-F2	94.86(13)
O9-Ga1-O1#1	92.57(13)	F3-Ga3-O7	93.52(13)
O9#1-Ga1-O1#1	87.43(13)	F2-Ga3-O7	167.36(9)
O9-Ga1-O1	87.43(13)	F3-Ga3-O8	89.19(13)
O9#1-Ga1-O1	92.57(13)	F2-Ga3-O8	84.22(12)
O1#1-Ga1-O1	180.0	O7-Ga3-O8	86.46(12)
O9-Ga1-F1#2	87.29(14)	F3-Ga3-O3#3	86.63(13)
O9#1-Ga1-F1#2	92.71(14)	F2-Ga3-O3#3	90.99(11)
O1#1-Ga1-F1#2	85.10(10)	O7-Ga3-O3#3	98.93(12)
O1-Ga1-F1#2	94.90(10)	O8-Ga3-O3#3	173.36(10)
O9-Ga1-F1#3	92.71(14)	F3-Ga3-F1	175.29(8)
O9#1-Ga1-F1#3	87.29(14)	F2-Ga3-F1	84.89(12)
O1#1-Ga1-F1#3	94.90(10)	O7-Ga3-F1	87.52(13)
O1-Ga1-F1#3	85.10(10)	O8-Ga3-F1	95.46(13)
F1#2-Ga1-F1#3	180.0	O3#3-Ga3-F1	88.67(12)
O6-Ga2-O4	106.69(13)	O7-P1-O9#3	113.7(2)
O6-Ga2-O5	107.57(14)	O7-P1-O6	105.94(15)
O4-Ga2-O5	105.32(12)	O9#3-P1-O6	109.3(2)
O6-Ga2-O2#4	107.52(14)	O7-P1-O5#5	111.16(15)
O4-Ga2-O2#4	108.45(14)	O9#3-P1-O5#5	108.23(15)
O5-Ga2-O2#4	120.55(12)	O6-P1-O5#5	108.38(15)
O1-P2-O3	113.9(2)	O1-P2-O2	108.5(2)
O1-P2-O4	111.6(2)	O3-P2-O2	108.5(2)
O3-P2-O4	107.4(2)	O4-P2-O2	106.7(2)
P2-O1-Ga1	128.3(2)	P1#5-O5-Ga2	130.0(2)
P2-O2-Ga2#4	123.2(2)	P1-O6-Ga2	137.9(2)
P2-O3-Ga3#3	137.1(2)	P1-O7-Ga3	135.5(2)
P2-O4-Ga2	150.6(2)	P1#3-O9-Ga1	128.5(2)
Ga3-F1-Ga1#6	130.38(12)		

[a] Symmetry transformation used to generate equivalent atoms: #1: $-x$, $-y+1$, $-z$; #2: $x-1$, y, z; #3: $-x+1$, $-y+1$, $-z$; #4: $-x$, $-y$, $-z$; #5: $-x+1$, $-y$, $-z$.

anisotropic displacement parameters, leading to the reliability factors: $R_1=0.0304$ ($R_1=\Sigma||F_o|-|F_c||/\Sigma|F_o|$) and $\omega R_2=0.0652$ ($R_2=\{\Sigma\omega(F_o^2-F_c^2)^2/\Sigma\omega(F_o^2)^2\}^{1/2}$) for all data.

The simulated XRD pattern of Mu-23 calculated from structure data (Figure 2b) fits the experimental one well. According to the elemental and microprobe analyses, the as-

0947-6539/02/0807-1616 $ 20.00+.50/0 *Chem. Eur. J.* **2002**, *8*, No. 7

synthesized Mu-23 sample had the following composition (wt.%): Ga 29.2, P 10.5, F 10.0, N 4.6, C 12.2; this is in good agreement with the theoretical composition obtained from the unit cell formula $[(C_6H_{15}N_2)(C_6H_{16}N_2)Ga_5F_6(H_2O)_2(PO_4)_4]\cdot 4H_2O$ found by structure determination: Ga 29.5, P 10.5, F 9.7, N 4.7, C 12.2.

The thermal behavior of Mu-23 was investigated by high-temperature XRD analysis and TG/DTA thermal analyses. The total weight loss occurs in three steps (Figure 3). The first,

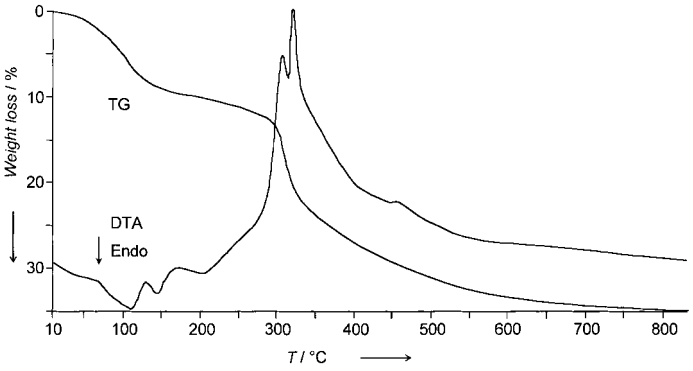

Figure 3. Thermal analyses (TG, DTA) under air of the hydroxygallophosphate Mu-23.

below 200 °C (10 wt.%), corresponds to the removal of water, as confirmed by the presence of endothermic peaks on the DTA curve in the same temperature range. The second step, between 200 and 850 °C (25 wt.%), corresponds to the partial decomposition of the organic template and removal of hydrofluoric acid; the removal of the amine results in a collapse of the structure. From high-temperature XRD analysis, amorphization is observed at 250 °C (lower heating rate). After heating at 850 °C the sample is still black, because of traces of organic compounds. Their removal occurs only at 1000 °C (3 wt.%) and then the resulting white material corresponds to a cristobalite-type gallophosphate. The total weight loss observed between 10 and 1000 °C is close to 38 wt.%, in good agreement with the amount of water, template, and fluorine found by crystal structure determination and chemical analysis (38.9 wt.%).

Structure description: Mu-23 consists of amine and water molecules intercalated between inorganic sheets. The presence of Ga1-F1-Ga3 bridges with Ga–F distances of about 1.95 Å was revealed first. For Ga3, which has three terminal groups (F, OH, or H_2O), the two shortest bond lengths, 1.854(3) and 1.885(3) Å, were attributed to terminal F atoms F2 and F3, respectively. Such bond lengths have previously been observed in other fluorogallophosphates: ULM-9 (1.800(2) Å),[17] Ga-PO_4-CJ2 (1.903(2) Å),[18] TMP-GaPO (1.79(2) Å),[19] pseudo-KTP-type gallophosphate (1.900(3) Å),[20] and Mu-15 (1.86(1) Å).[21] The remaining bond length, 1.921(3) Å, was attributed to Ga3–O8H or Ga3–$O8H_2$. According to the bond valence calculation[22] (see Table 7), the latter (Ga3–$O8H_2$) is more probable. This assignment of the different terminal groups (2 F and H_2O) seems to be confirmed by the hydrogen bonding scheme (below). Moreover, an F/H_2O molar ratio of two on these terminal positions is expected from the chemical and microprobe analyses (a total of six F atoms per unit cell). However, a mixture of F atoms and water molecules on these three terminal positions cannot be excluded.

Table 7. Bond valence analysis of the gallophosphate Mu-23, according to Ref. [22].

Atoms	H[a]	Ga1	Ga2	Ga3	P1	P2	Σs[b]	Expected valence
O1		0.55				1.29	1.84	2
O2			0.76			1.13	1.89	2
O3				0.57		1.28	1.85	2
O4			0.80			1.22	2.02	2
O5			0.78		1.17		1.95	2
O6			0.81		1.20		2.01	2
O7				0.60	1.29		1.89	2
O8	0.8 × 2			0.57			2.17	2
O9		0.60			1.28		1.88	2

[a] On the basis of an O–H bond length of 0.96 Å. [b] Calculated from the equation: $s = \exp[(R_0 - d)/B]$, with d = experimental distance, $R_0 = 1.62$, $B = 0.36$ for P–O and $R_0 = 1.73$, $B = 0.38$ for Ga–O.

Therefore, layers display $GaO_2F_3(H_2O)$ and GaO_4F_2 octahedra, and GaO_4 and two crystallographically different PO_4 tetrahedra. The GaO_4F_2, GaO_4, and PO_4 polyhedra are quite regular. Their average bond lengths are d(Ga1–O) ≈ 1.94 Å, d(Ga2–O) ≈ 1.82 Å, d(P1–O) ≈ 1.53 Å, and d(P2–O) ≈ 1.53 Å. The $GaO_2F_3(H_2O)$ octahedron is more distorted because of the presence of terminal groups (d(Ga3–X) (X = F or H_2O) ranges from 1.85 to 1.92 Å).

In the asymmetric unit of Mu-23 (Figure 4), all the remaining atoms are in general positions, except for Ga(1) which is located on the inversion center. The inorganic sheet

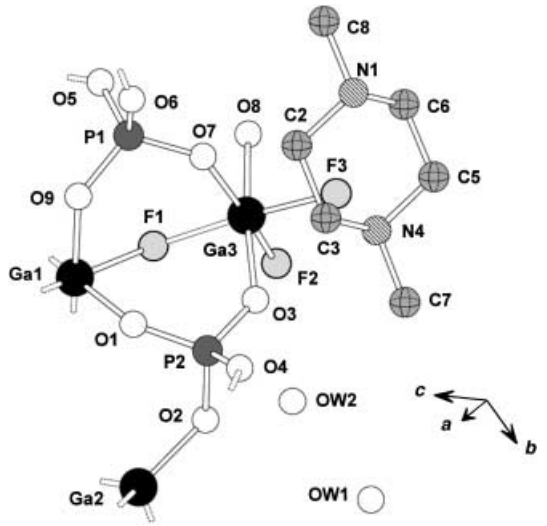

Figure 4. Asymmetric unit of Mu-23 (H atoms are not reported).

consists of four-membered ring ladder chains running along the [1 0 0] direction (bold lines, Figure 5) and eight-membered rings. This type of zigzag chain has previously been described as a $[Z(3,3)]_\infty$ chain by Ozin et al.[23] The unusual feature of Mu-23 is the connectivity scheme of its $[Z(3,3)]_\infty$ chains. The

bonding of the Ga1 atoms through F to two Ga3 atoms ensures the connection of the chains and leads to the formation of the layers. This connection unit is built of Ga_2PO_2F groups and forms three-membered rings (hatched area, Figure 5).

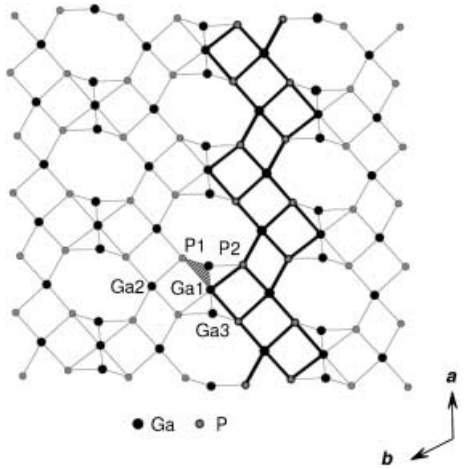

Figure 5. Projection of the structure of Mu-23 in the plane (001) showing the eight-membered rings and the four-membered ring ladder chains (thick lines). For clarity, the amine and water molecules, and the framework O and F atoms are omitted.

The F2 and F3 atoms and the oxygen atom O8 of the water molecule bound to Ga3 protrude into the interlayer space. It is noteworthy that O8 is bound only through hydrogen interactions to water molecules located in the interlayer space (Figure 6). Apart from F2, which interacts with OW1, the F atoms interact mainly with the organic amine. The corresponding bond lengths are reported in Table 5. Such hydrogen-bonding interactions (O8 with water, and F atoms mainly with the protonated N atoms of the template) reinforce the hypothesis that one of these terminal atoms is not fluorine. This is also in agreement with the chemical and microprobe analyses.

Solid-state NMR spectroscopy

^{31}P NMR spectroscopy: The two signals at $\delta = -7.2$ and -9.2 (Figure 7) in the ^{31}P magic angle spinning (MAS) NMR spectrum of Mu-23, with an intensity ratio close to 1:1, reveals the existence of two distinct crystallographic phosphorus sites with the same multiplicity, in agreement with the structure determination. No significant change in the relative intensity of the two peaks was observed in CP MAS NMR experiments with different contact times, showing that the two types of P atom have similar hydrogen environments.

^{13}C NMR spectroscopy: The ^{13}C CP MAS NMR spectrum displays three different signals at $\delta = 50.8$, 45.1, and 43.1 (Figure 8). The signal at $\delta = 50.8$ was assigned to the CH_2 groups. The other two signals correspond to the two distinct crystallographic methyl groups of mono- and diprotonated amines. However, the chemical shifts observed for these two

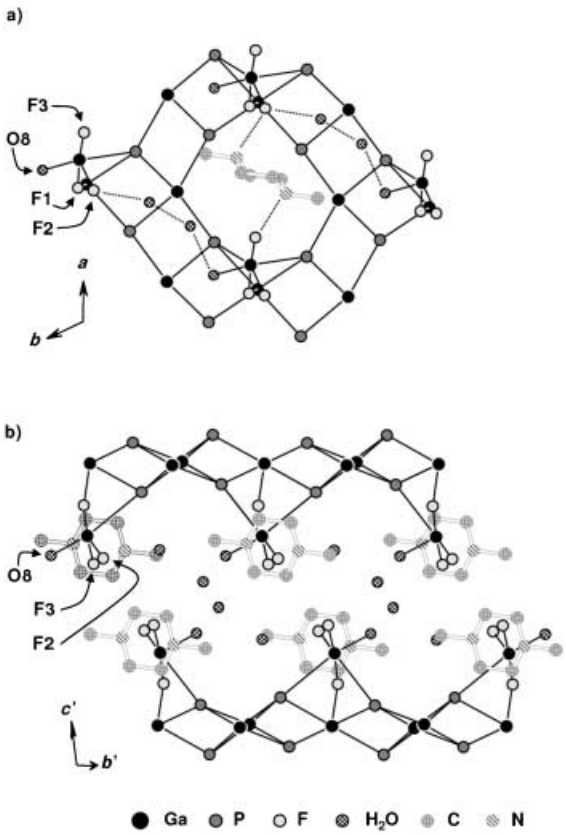

Figure 6. a) View towards the (001) plane showing the hydrogen bonds (broken lines). b) View along the *a* axis of the structure of Mu-23 showing the amine and water molecules intercalated between the inorganic layers. H atoms are omitted for clarity. $c' = c\cos(\beta - 90)$; $b' = b\cos(\gamma - 90)$.

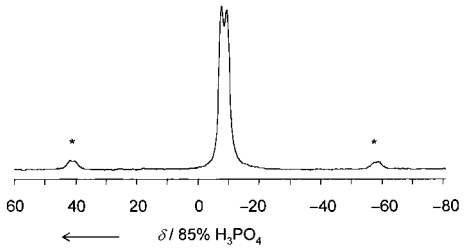

Figure 7. ^{31}P MAS NMR spectrum of the fluorogallophosphate Mu-23 (* spinning side bands).

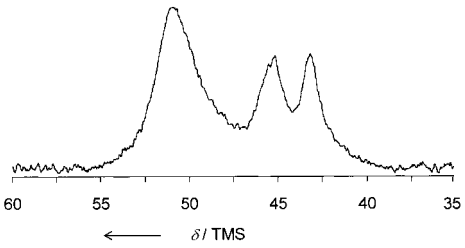

Figure 8. ^{13}C CP MAS NMR spectrum of the fluorogallophosphate Mu-23.

signals are slightly different from the ^{13}C liquid NMR values expected for mono- and diprotonated amines.

^{19}F NMR spectroscopy: In the ^{19}F MAS NMR spectrum of Mu-23, the main signal is observed at $\delta = -130.7$ and a shoulder is clearly evident at about $\delta = -139$ (Figure 9). These chemical shifts correspond with those usually observed

0947-6539/02/0807-1618 $ 20.00+.50/0 *Chem. Eur. J.* **2002**, *8*, No. 7

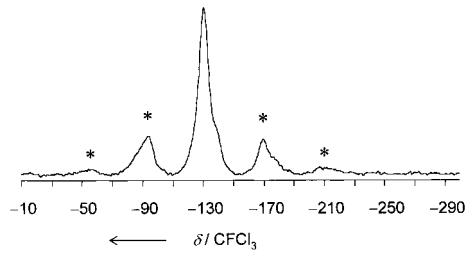

Figure 9. ^{19}F MAS NMR spectrum of the fluorogallophosphate Mu-23.

for bridging and terminal F atoms. From this spectrum, however, it is difficult to distinguish the different types of fluorine present in the material, since the relative intensity ratio of the two components (5:1) does not fit with that expected from the structure analysis (2:1).

Conclusion

The use of 1,4-dimethylpiperazine as a structure-directing agent in the $Ga_2O_3/P_2O_5/HF/H_2O$ system was investigated. A new layered fluorogallophosphate, $[(C_6H_{15}N_2)(C_6H_{16}N_2)\text{-}Ga_5F_6(H_2O)_2(PO_4)_4]\cdot 4H_2O$ (Mu-23) was obtained; it crystallized within a very narrow range of experimental conditions.

The structure of this new material consists of inorganic sheets built from four-membered ring ladder chains connected to each other through three-membered Ga_2PO_2F units. Protonated amines and water molecules localized in the interlayer space have strong hydrogen-bonding interactions with the terminal water or fluorine groups of the inorganic framework. Such interactions ensure the cohesion of the structure, which collapses after calcination at 250 °C.

This fluorogallophosphate is characterized by an unusual Ga/P ratio of 5:4. To our knowledge, Mu-23 is the first layered gallophosphate with a Ga/P ratio higher than one.

Experimental Section

Synthesis: For the synthesis mixture, the gallium source was an amorphous gallium oxyhydroxide (GaOOH) that was prepared by heating a gallium nitrate aqueous solution (Rhône-Poulenc) at 250 °C for 24 h. The other reactants were orthophosphoric acid (Labosi, 85 %), hydrofluoric acid (Carlo Erba, 40 %) and 1,4-dimethylpiperazine (DMPIP) (Aldrich, 98 %). The batch molar composition was $Ga_2O_3/P_2O_5/HF/H_2O/DMPIP = 1:4:8:640:8$. The mixture was prepared by adding the phosphoric acid (0.58 g, 5 mmol) to a stirred suspension of GaOOH (0.14 g, 1.3 mmol) in deionized water (6.86 g, 390 mmol). The mixture was homogenized for 10 min before successive addition of hydrofluoric acid (0.26 g, 5 mmol) and of amine (0.58 g, 5 mmol). The mixture was aged, while being stirred, for 1 h at room temperature and transferred to a 40 mL PTFE-lined stainless steel autoclave. The crystallization occurred under static conditions at 130 °C for six days. The initial and final pH values of the mixture were 5. After cooling, the product was recovered, washed with deionized water, and dried at 60 °C overnight.

Characterization techniques: The morphology and size of the crystals were determined by scanning electron microscopy with a Philips XL30 microscope.

The powder XRD patterns were obtained with $Cu_{K\alpha 1}$ radiation on a STOE STADI-P diffractometer equipped with a curved germanium (111) primary monochromator and a linear position-sensitive detector. High-temperature XRD was performed using a variable-temperature photographic chamber (Huber, model 631) attached to the same X-ray generator ($Cu_{K\alpha_1}$ radiation) in which the sample was kept in a flow of dry air.

Single-crystal XRD was carried out with $Mo_{K\alpha}$ radiation in ω scan mode on a Syntex $P2_1$ four-circle diffractometer equipped with a graphite monochromator. CCDC 172031 contains the supplementary crystallographic data for this paper. These data can be obtained free of charge via www.ccdc.cam.ac.uk/conts/retrieving.html (or from the Cambridge Crystallographic Data Centre, 12 Union Road, Cambridge CB2 1EZ, UK; fax: (+44) 1223-336033; or deposit@ccdc.cam.uk).

The Ga and P analyses were performed by inductively coupled plasma emission spectroscopy. After mineralization of the as-synthesized sample, fluorine content was determined by using a fluoride ion-selective electrode. C and N content were determined by coulometric and catharometric methods respectively, after calcination of the sample.

The Ga, P and F contents were confirmed by microprobe analysis on a Castaing-type (Camebax) scanning electron microscope.

Thermogravimetric (TGA) and differential thermal analyses (DTA) were performed under air on a Setaram Labsys thermoanalyzer with a heating rate of 5 °C min^{-1} up to 850 °C. At this final temperature, a gray residue was obtained. Calcination at 1000 °C was necessary to obtain a white product and, therefore, the total removal of the organic template.

The ^{13}C CP MAS NMR spectrum was recorded on a Bruker MSL 300 spectrometer and ^{31}P and ^{19}F NMR spectra on a Bruker DSX 400 spectrometer. The recording conditions are given in Table 8.

Table 8. Conditions for recording the NMR spectra.

	^{13}C	^{31}P		^{19}F
	CP MAS	MAS	CP MAS	MAS
chemical shift standard	TMS	85 % H_3PO_4	85 % H_3PO_4	$CFCl_3$
frequency [MHz]	75.47	161.98	161.98	376.45
pulse width [μs]	3.7	4.5	4.5	8.2
flip angle	$\pi/2$	$\pi/2$	$\pi/2$	$\pi/2$
contact time [ms]	1	–	0.1 and 1	–
recycle time [s]	6.5	500	10	20
spinning rate [kHz]	4	8	8	14
number of scans	426	12	32	32

Acknowledgements

The authors thank the Institut Français du Pétrole (IFP), which kindly provided the gallium nitrate source.

[1] S. J. Miller (Chevron Research Co.), EP 209997, **1987** [*Chem. Abstr.* **1987**, *106*, 105235r].
[2] a) M. E. Davis, C. Saldarriaga, C. Montes, J. Garcès, C. Crowder, *Zeolites* **1988**, *8*, 362–366; b) L. B. McCusker, C. Baerlocher, E. Jahn, M. Bülow, *Zeolites* **1991**, *11*, 308–313.
[3] Q. Huo, R. Xu, S. Li, Z. Ma, J. M. Thomas, R. H. Jones, A. M. Chippindale, *J. Chem. Soc. Chem. Commun.* **1992**, 875–876.
[4] C. H. Lin, S. L. Wang, K. H. Lii, *J. Am. Chem. Soc.* **2001**, *123*, 4649–4650.
[5] G. Y. Yang, S. C. Sevov, *J. Am. Chem. Soc.* **1999**, *121*, 8389–8390.
[6] J. L. Guth, H. Kessler, R. Wey, *New Developments in Zeolite Science and Technology* (Eds.: Y. Murakami, A. Lijima, J. W. Ward), Kodansha–Elsevier, Tokyo, **1986**, pp. 121–128.
[7] A. Choudhury, S. Natarajan, C. N. R. Rao, *Chem. Commun.* **1999**, 1305–1306.
[8] N. Guillou, Q. Gao, M. Nogues, R. E. Morris, M. Hervieu, G. Férey, A. K. Cheetham, *C. R. Acad. Sci. Ser. IIc* **1999**, 387–392.
[9] a) M. Estermann, L. B. McCusker, C. Baerlocher, A. Merrouche, H. Kessler, *Nature* **1991**, *352*, 320–323; b) A. Merrouche, J. Patarin, H. Kessler, M. Soulard, L. Delmotte, J. L. Guth, J. F. Joly, *Zeolites* **1992**, *12*, 226–232.
[10] M. P. Attfield, R. E. Morris, E. Gutierrez-Puebla, A. Monge-Bravo, A. K. Cheetham, *J. Chem. Soc. Chem. Commun.* **1995**, 843–844.
[11] C. Y. Chen, P. Chu, K. H. Lii, *Chem. Commun.* **1999**, 1473–1474.

  0947-6539/02/0807-1619 $ 20.00+.50/0

[12] T. Wessels, L. B. McCusker, C. Baerlocher, P. Reinert, J. Patarin, *Microporous Mesoporous Mater.* **1998**, *23*, 67 – 77.
[13] T. Loiseau, G. Férey, *Eur. J. Solid State Inorg. Chem.* **1993**, *30*, 369 – 381.
[14] S. J. Weigel, R. E. Morris, G. D. Stucky, A. K. Cheetham, *J. Mater. Chem.* **1998**, *8*, 1607 – 1611.
[15] G. M. Sheldrick, SHELXS-86, Program for the Solution of Crystal Structures, University of Göttingen, Germany, **1986**.
[16] G. M. Sheldrick, SHELXL-93, Program for Crystal Structure Determination, University of Göttingen, Germany, **1993**.
[17] D. Riou, G. Férey, *Eur. J. Solid State Inorg. Chem.* **1994**, *31*, 605 – 613.
[18] G. Férey, T. Loiseau, P. Lacorre, F. Taulelle, *J. Solid State Chem.* **1993**, *105*, 179 – 190.
[19] V. Munch, F. Taulelle, T. Loiseau, G. Férey, A. K. Cheetham, S. Weigel, G. D. Stucky, *Magn. Reson. Chem.* **1999**, *37*, S100 – S107.
[20] T. Loiseau, C. Paullet, N. Simon, V. Munch, F. Taulelle, G. Férey, *Chem. Mater.* **2000**, *12*, 1393 – 1399.
[21] A. Matijasic, J.-L. Paillaud, J. Patarin, *J. Mater. Chem.* **2000**, *10*, 1345 – 1351.
[22] I. D. Brown, in *Structure and Bonding in Crystals*, *Vol. 2* (Eds.: M. O'Keeffe, A. Navrotsky), Academic Press, New York, **1981**, Chapter 14, pp. 1 – 30.
[23] S. Oliver, A. Kuperman, G. A. Ozin, *Angew. Chem.* **1998**, *110*, 48 – 64; *Angew. Chem. Int. Ed.* **1998**, *37*, 47 – 62.

Received: October 11, 2001 [F3605]

  0947-6539/02/0807-1620 $ 20.00+.50/0